

# Interim Design Report

Micromouse Sensing Subsystem



**Prepared by:**

Richard Mabvirakare

**Prepared for:**

EEE3088F

Department of Electrical Engineering  
University of Cape Town

May 18, 2024

# Declaration

1. I know that plagiarism is wrong. Plagiarism is to use another's work and pretend that it is one's own.
2. I have used the IEEE convention for citation and referencing. Each contribution to, and quotation in, this report from the work(s) of other people has been attributed, and has been cited and referenced.
3. This report is my own work.
4. I have not allowed, and will not allow, anyone to copy my work with the intention of passing it off as their own work or part thereof.

---

R.Mabvirakare

May 18, 2024

---

Name Surname

---

Date

# Contents

<b>1</b>	<b>Introduction</b>	<b>1</b>
1.1	Problem Description . . . . .	1
1.2	Scope and Limitations . . . . .	1
1.3	GitHub Link . . . . .	1
<b>2</b>	<b>Requirements Analysis</b>	<b>2</b>
2.1	Requirements . . . . .	2
2.2	Specifications . . . . .	2
2.3	Testing Procedures . . . . .	3
2.4	Traceability Analysis . . . . .	3
2.4.1	Traceability Analysis 1 . . . . .	4
2.4.2	Traceability Analysis 2 . . . . .	4
2.4.3	Traceability Analysis 3 . . . . .	4
2.4.4	Traceability Analysis 4 . . . . .	4
2.4.5	Traceability Analysis 5 . . . . .	4
<b>3</b>	<b>Subsystem Design</b>	<b>5</b>
3.1	Design Decisions . . . . .	5
3.1.1	Component Selection . . . . .	5
3.1.2	Unique Designs . . . . .	6
3.1.3	Final Design . . . . .	7
3.2	Failure Management . . . . .	10
3.3	System Integration and Interfacing . . . . .	10
<b>4</b>	<b>Acceptance Testing</b>	<b>12</b>
4.1	Tests . . . . .	12
4.2	Critical Analysis of Testing . . . . .	13
4.2.1	AT-01: Functionality Test of the ER Subsystems . . . . .	13
4.2.2	AT-02: Consistency Test of the Sensing Subsystem's Output Voltage . . . . .	14
4.2.3	AT-03: Functionality Test of the Sensing Subsystem Software . . . . .	15
4.2.4	AT-04: Power Consumption Test of the Sensing Subsystem . . . . .	15
4.2.5	AT-05: Physical Compatibility Test . . . . .	16
<b>5</b>	<b>Conclusion</b>	<b>17</b>
5.1	Recommendations . . . . .	18
	<b>Bibliography</b>	<b>19</b>

# Chapter 1

## Introduction

### 1.1 Problem Description

The micro-mouse project aims to design and construct subassemblies for a simplified maze-solving robot. The project is divided into four modules: processor, motherboard, sensing, and power. Working in pairs, each student is responsible for designing either the sensing or power subsystem. The objective is to create a functional micro-mouse that navigates a maze while adhering to a strict budget and meeting the specified requirements for each subsystem. The sensing subsystem, which is the focus of this report, plays a crucial role in detecting obstacles and walls, enabling the micro-mouse to navigate the maze effectively.

### 1.2 Scope and Limitations

The scope of this project is limited to the design and implementation of the sensing subsystem for the micro-mouse robot. The subsystem will be designed to detect obstacles and walls, incorporate power-saving features, and interface with the processor board. The sensing subsystem's design will cover its integration with the other modules. However, the overall navigation algorithm for the micro-mouse is beyond the scope of this project.

The project's limitations include the strict budget constraints, which may impact component selection and design choices. Additionally, the sensing subsystem's performance may be affected by factors such as sensor accuracy, ambient light conditions, and battery life. Testing and development may also be limited by the availability of resources and time constraints.

### 1.3 GitHub Link

<https://github.com/max035/EEE3088F-Micro-Mouse> -----

# Chapter 2

## Requirements Analysis

### 2.1 Requirements

The requirements for a micromouse sensing module are described in [Table 2.1](#).

Table 2.1: User and functional requirements of the sensing subsystem.

Requirement ID	Description
R-01	The sensing subsystem must include sensors capable of detecting walls within a suitable range for maze navigation
R-02	The sensing subsystem must provide reliable and consistent wall detection, mitigating the effects of ambient light on detection accuracy.
R-03	The sensing subsystem must include software that processes the sensor data, indicating the presence of walls on the left, right, and front of the micro-mouse.
R-04	The sensing subsystem must use a power-saving mechanism to reduce overall power consumption.
R-05	The sensing subsystem must fit within the available space on the micro-mouse chassis and connect to the 2x14 pin header on the motherboard.

### 2.2 Specifications

The specifications, refined from the requirements in [Table 2.1](#), for the micromouse power module are described in [Table 2.2](#).

### 2.3. Testing Procedures

Table 2.2: Specifications of the sensing subsystem derived from the requirements in [Table 2.1](#).

Specification ID	Description
SPEC-01	The sensing subsystem shall detect walls on the left, right, and front of the micro-mouse, each with a detection range of 100mm to 200mm, conforming to the size of the maze block being 200mm x 200mm.
SPEC-02	The sensing subsystem shall produce a consistent output voltage or voltage range that is minimally affected by environmental factors to ensure reliable wall detection.
SPEC-03	The sensing subsystem shall include software that reads and interprets sensor data sent by the sensors' output to indicate the presence of walls on the left, right, and front of the micro-mouse, by toggling the PB7, PB5, and PB6 LEDs of the microcontroller, respectively.
SPEC-04	The sensing subsystem shall use a power-saving mechanism that reduces power consumption to 50% or lower compared to standard continuous operation.
SPEC-05	The sensing subsystem PCB shall fit within the available space on the micro-mouse chassis, with a width less than 70mm (from one wheel to the next) and a length greater than 6mm to accommodate the 2x14 connector and less than 50mm to ensure the micro-mouse can navigate the maze effectively.

## 2.3 Testing Procedures

A summary of the testing procedures detailed in [chapter 4](#) is given in [Table 2.3](#).

Table 2.3: Acceptance Test

Acceptance Test ID	Description
AT-01	Verify that the ER subsystems can detect walls within the specified range of 100mm to 200mm.
AT-02	Test the consistency of the sensing subsystem's output voltage under varying environmental conditions using the analog to digital logic converter.
AT-03	Verify that the sensing subsystem software processes sensor data and indicates the presence of walls by toggling the corresponding LEDs on the microcontroller.
AT-04	Test the power consumption of the sensing subsystem to verify that the PWM power-saving mechanism reduces power consumption by 50% or more compared to continuous operation.
AT-05	Ensure that the sensing subsystem PCB fits within the specified dimensions and connects properly to the 2x14 pin header on the motherboard.

## 2.4 Traceability Analysis

The show how the requirements, specifications and testing procedures all link, [Table 2.4](#) is provided.

Table 2.4: Requirements Traceability Matrix

#	Requirements	Specifications	Acceptance Test
1	R-01	SPEC-01	AT-01
2	R-02	SPEC-02	AT-02
3	R-03	SPEC-03	AT-03
4	R-04	SPEC-04	AT-04
5	R-05	SPEC-05	AT-05

#### 2.4.1 Traceability Analysis 1

R-01 is satisfied by SPEC-01, which states that the sensing subsystem shall detect walls on the left, right, and front of the micro-mouse, each with a detection range of 100mm to 200mm, conforming to the size of the maze block being 200mm x 200mm. This requirement is verified by AT-01, where the ER subsystems are tested to ensure they can detect walls within the specified range.

#### 2.4.2 Traceability Analysis 2

R-02 is satisfied by SPEC-02, which states that the sensing subsystem shall produce a consistent output voltage or voltage range that is minimally affected by environmental factors to ensure reliable wall detection. This requirement is verified by AT-02, which tests the consistency of the sensing subsystem's output voltage under varying environmental conditions using the analog to digital logic converter.

#### 2.4.3 Traceability Analysis 3

R-03 is satisfied by SPEC-03, which states that the sensing subsystem shall include software that reads and interprets sensor data sent by the sensors' output to indicate the presence of walls on the left, right, and front of the micro-mouse, by toggling the PB7, PB5, and PB6 LEDs of the microcontroller, respectively. This requirement is verified by AT-03, which checks that the sensing subsystem software processes sensor data and indicates the presence of walls by toggling the corresponding LEDs on the microcontroller.

#### 2.4.4 Traceability Analysis 4

R-04 is satisfied by SPEC-04, which states that the sensing subsystem shall use a power-saving mechanism that reduces power consumption to 50% or lower compared to standard continuous operation. This requirement is verified by AT-04, which tests the power consumption of the sensing subsystem to verify that the PWM power-saving mechanism reduces power consumption by 50% or more compared to continuous operation.

#### 2.4.5 Traceability Analysis 5

R-05 is satisfied by SPEC-05, which states that the sensing subsystem PCB shall fit within the available space on the micro-mouse chassis, with a width less than 70mm (from one wheel to the next) and a length greater than 6mm to accommodate the 2x14 connector and less than 50mm to ensure the micro-mouse can navigate the maze effectively. This requirement is verified by AT-05, which ensures that the sensing subsystem PCB fits within the specified dimensions and connects properly to the 2x14 pin header on the motherboard.

# Chapter 3

## Subsystem Design

### 3.1 Design Decisions

The design decisions for the sensing subsystem were made based on careful consideration of component options, power-saving mechanisms, output and level shifting, and PCB layout and routing.

#### 3.1.1 Component Selection

Table 3.1: Summary of Component Selection

Component	Options Considered	Pros	Cons	Final Selection
IR Emitting Diode	<ul style="list-style-type: none"><li>• TSAL6100</li><li>• TSAL6200</li><li>• TSAL4400</li></ul>	<ul style="list-style-type: none"><li>• All work well at 100mA current, consuming less power</li><li>• All suitable for desired sensing distance</li><li>• Familiarity with TSAL6100 due to breadboard assignment</li></ul>	<ul style="list-style-type: none"><li>• Limited stock availability on JLCPCB for TSAL6100 and TSAL6200</li><li>• TSAL4400 senses IR light from its top, unlike TSAL6100 and TSAL6200</li></ul>	TSAL4400 - Reason: Component availability
Photodiode	<ul style="list-style-type: none"><li>• SFH205FA</li><li>• SFH203PFA</li></ul>	<ul style="list-style-type: none"><li>• Suitable for side-facing detection</li><li>• Both work well with 100k resistor in reverse bias configuration</li><li>• Familiarity with SFH205FA due to breadboard assignment</li></ul>	<ul style="list-style-type: none"><li>• Limited stock availability on JLCPCB for SFH205FA</li><li>• SFH203 senses IR light from its top, unlike SFH205FA</li></ul>	SFH203PFA - Reason: Component availability
Phototransistor	<ul style="list-style-type: none"><li>• QRD113</li><li>• QRD114</li></ul>	<ul style="list-style-type: none"><li>• Suitable for short-distance applications</li><li>• Good stock availability on JLCPCB</li></ul>	<ul style="list-style-type: none"><li>• Not suitable for long-distance sensing required in this project</li></ul>	Not selected - Reason: Component availability

**Note:** Due to limited stock at JLCPCB, the TSAL4400 and SFH203PFA were used instead of the originally selected TSAL6100 and SFH205FA. This change, made later in the project, means that the report's calculations and assumptions are based on the initially selected components. This oversight was a critical mistake. However, the TSAL4400 and SFH203PFA are functionally similar to the original components, ensuring project success. Additionally, the IR emitter-receiver combination was chosen over phototransistors (QRD113 and QRD114) for its superior performance in long-distance sensing.

## Calculations

### Emitter Circuit Calculations

From the TSAL6100 datasheet:

- Voltage drop,  $V_f = 1.5 \text{ V}$
- Typical current of the emitting diode is  $100 \text{ mA}$

Applying Kirchhoff's Voltage Law and solving for the resistor value:

$$R = \frac{V_{in} - V_f}{I} = \frac{3.3 \text{ V} - 1.5 \text{ V}}{100 \text{ mA}} = 18 \Omega$$

### Receiver Circuit Calculations

The resistor value for the receiver was determined experimentally during the breadboard assignment:

- A  $10 \text{ k}\Omega$  resistor produced outputs in the 100s millivolt region (no obstacle) and increased to around  $3 \text{ V}$  as the obstacle approached.
- A  $100 \text{ k}\Omega$  resistor produced outputs above  $1 \text{ V}$  with no obstacle and a gradual, clear voltage increase to  $3.3 \text{ V}$  as the obstacle came closer.

Therefore, a  $100 \text{ k}\Omega$  resistor will be used in series with the SFH205FA photodiode.

### 3.1.2 Unique Designs

**Unique Design Decision 1: Analog to Digital Logic Converter** After obtaining the analog output signal from the emitter-receiver (ER) sensor, the next step was to process and interpret this data for wall detection. Instead of using an Analog-to-Digital Converter (ADC), which can be complex and resource-intensive, a level shifter was implemented to convert the analog signal to digital logic levels.

The level shifter acts as an analog to digital logic converter, where voltages less than  $0.7\text{V}$  produce a  $0\text{V}$  output, and voltages greater than  $0.7\text{V}$  produce a  $3.3\text{V}$  output.

This design decision offers several advantages:

1. Simplified interfacing between the sensing subsystem and the processor.
2. Reduced software complexity by eliminating the need for complex ADC implementation and signal processing.
3. Resource optimization by conserving processing power and memory resources.

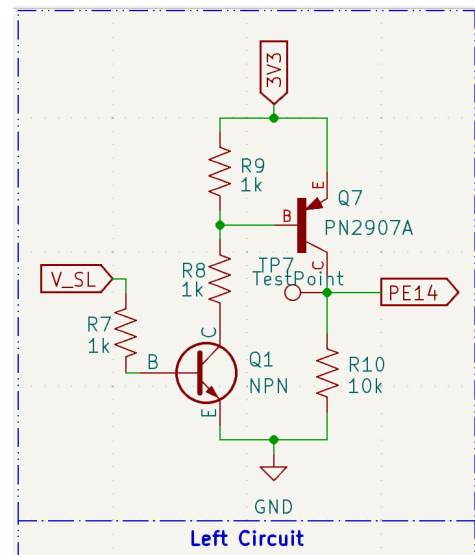


Figure 3.1: Schematic

By employing a level shifter as an analog to digital logic converter, the sensing subsystem can effectively provide wall detection information to the processor in a simplified and resource-efficient manner.

### Unique Design Decision 2: PCB Shape Modification for Sensor Placement

The provided template for the sensing subsystem PCB design posed a challenge, as the left and right sensors would be obstructed by the wheels of the micromouse. To overcome this issue, the PCB was extended forward just enough to ensure that the sensors were not obstructed while maintaining the micromouse's ability to fit within one block of the maze and minimizing the impact on the centre of gravity.

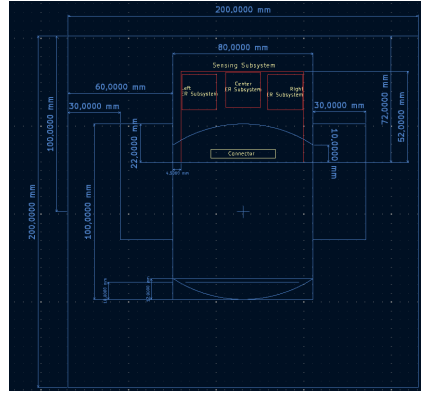


Figure 3.2: Schematic

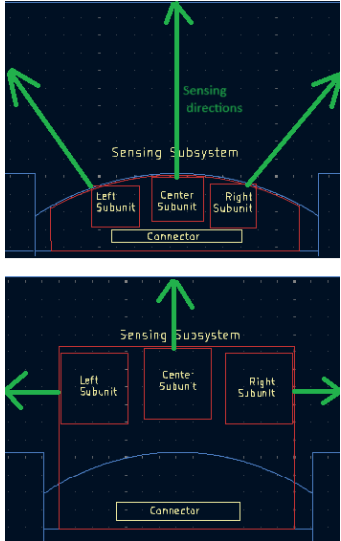


Figure 3.3: Schematic

An alternative solution considered was to rotate the sensors themselves to achieve the desired sensing angles while avoiding wheel obstruction. However, this approach was deemed potentially more complicated than extending the board, as it would have required additional mechanical fixtures and might not have provided reliable sensory data.

By extending the PCB forward, the sensors can be placed in front of the wheels without the need for rotation, ensuring unobstructed detection of walls on the left, right, and front of the micro-mouse. This design choice simplifies the assembly process and enhances the reliability of the sensory data.

**Unique Design Decision 3: Jumper for Potentiometer Calibration** To facilitate calibration of the ER sensor's output, a jumper was included in the design to allow for the connection of a potentiometer. This decision offers flexibility in calibrating the sensing subsystem without requiring significant hardware modifications. The jumper and potentiometer solution was chosen for its flexibility, simplicity, and cost-effectiveness in addressing the potential need for calibration in the sensing subsystem.

By incorporating a jumper for potentiometer calibration, the sensing subsystem gains the ability to adapt to varying environmental conditions and sensor characteristics, ensuring reliable wall detection performance. This design decision demonstrates a balance between flexibility, simplicity, and cost-effectiveness in addressing the potential need for calibration.

#### 3.1.3 Final Design

##### Power Saving Mechanism

Pulse Width Modulation (PWM) was selected to control the power supplied to the ER sensors, effectively reducing the overall power consumption of the sensing subsystem. This allows the ER sensors to operate for a shorter time while still functioning as intended, as long as the duty cycle is

### 3.1. Design Decisions

appropriately configured.

However, it is important to note that sourcing current directly from the GPIO pin may not be the best approach. A better solution would be to use a MOSFET switching circuit with PWM as the switch, and the circuit connected to the 3.7V battery for power. This would ensure that the GPIO pin is not overloaded, and the ER sensors receive adequate current.

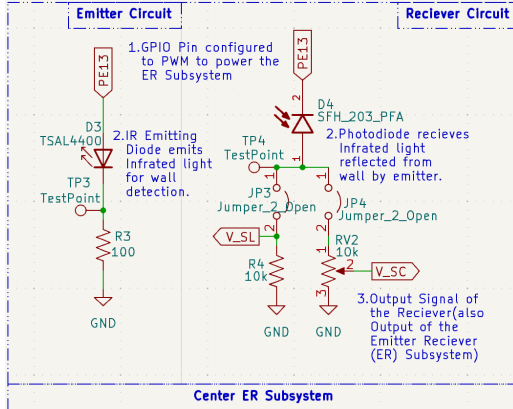


Figure 3.4: Current Implementation of PWM (without MOSFET Switching)

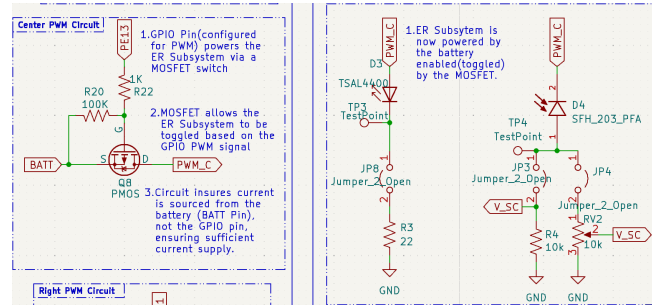


Figure 3.5: Better implementation of PWM (with MOSFET Switching)

The appropriate duty cycle will be determined during testing when the PCB is received.

### Output and Level Shifting

The analog output signals from the ER sensors need to be converted into a format that the processor could use to detect the presence of a wall and control an LED indicator. While an ADC could directly convert the analog signals for processing, a level shifting circuit offered a simpler solution. A level shifter translates signals between different voltage or logic levels, allowing the analog voltages from the ER sensors to be converted to digital levels compatible with the processor. This approach simplifies the interfacing between the sensing subsystem and the processor, enabling efficient wall detection and LED control without the need for a complex ADC solution.

Table 3.2: Summary of Design Decisions

Design Decision	Options Considered	Pros	Cons	Final Selection
Level Shifting	<ul style="list-style-type: none"> <li>NPN and PNP transistor-based level shifter</li> <li>MOSFET-based level shifter</li> </ul>	<ul style="list-style-type: none"> <li>Familiarity with transistors</li> <li>Transistors are easily sourced from White Lab if needed</li> <li>Transistors are less expensive than MOSFETs</li> <li>No current drawn at the gate from ER sensor output (for MOSFET)</li> </ul>	<ul style="list-style-type: none"> <li>Requires two transistors (for NPN and PNP)</li> <li>More expensive than transistors (for MOSFET)</li> </ul>	NPN and PNP transistor-based level shifter

To ensure that the level-shifting circuit would work reliably with the ER sensor outputs, simulations were conducted using LT Spice. The input into the level shifter was varied, confirming that voltages less than 0.7V resulted in approximately 0V output, while voltages greater than 0.7V resulted in

approximately 3.3V output. Additionally, the ER sensor's functionality had already been verified during the breadboard assignment.

## PCB Layout and Routing

Table 3.3: Summary of Design Decisions

Design Decision	Description	Rationale
Component Placement	<ul style="list-style-type: none"> <li>ER sensors placed to avoid obstruction by wheels</li> <li>PCB extended forward to accommodate ER sensors</li> </ul>	<ul style="list-style-type: none"> <li>Ensure unobstructed wall detection on left and right sides</li> <li>Maintain compact PCB size while allowing proper ER sensor functionality</li> </ul>
Routing	<ul style="list-style-type: none"> <li>Tracks placed and routed for all components</li> <li>Ground plane not included on top and bottom layers (mistake)</li> </ul>	<ul style="list-style-type: none"> <li>Ensure proper connectivity between components</li> <li>(Mistake) Thought tracks and routing would be sufficient without ground planes</li> </ul>

In hindsight, not including a ground plane on both the front and back of the board was a mistake. Ground planes offer several benefits, such as reducing noise and EMI, enhancing power delivery, facilitating improved thermal management, and simplifying routing.

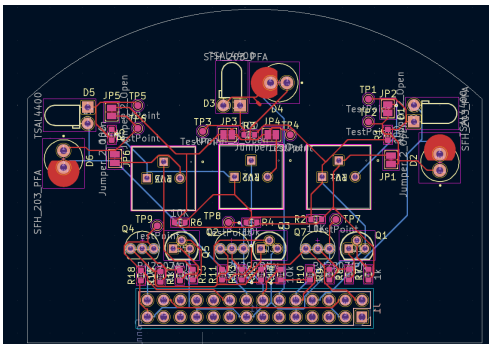


Figure 3.6: Current Implementation of PCB layout (without ground planes)

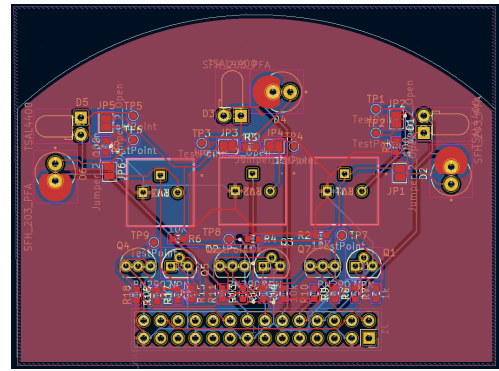


Figure 3.7: Better implementation of PCB layout (with ground planes)

## Final solution

The final solution for the sensing subsystem consists of three main components:

1. Emitter-Receiver (ER) Sensor Subsystem: Three separate ER circuits for left, front, and right wall detection, each using a TSAL4400 IR emitting diode and an SFH203 photodiode.
2. Power Saving Mechanism: Pulse Width Modulation (PWM) is used to reduce power consumption by controlling the duty cycle of the ER circuits.
3. Output and Level Shifting: An NPN and PNP transistor-based level shifter is used to convert the output signals from the ER circuits to digital levels suitable for the GPIO pins of the STM32 processor.

## 3.2. Failure Management

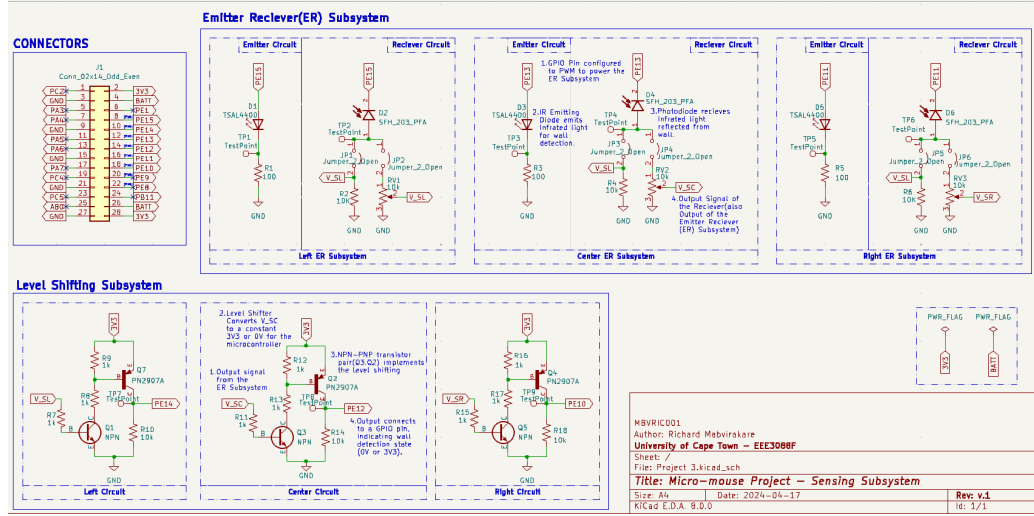


Figure 3.8: Schematic

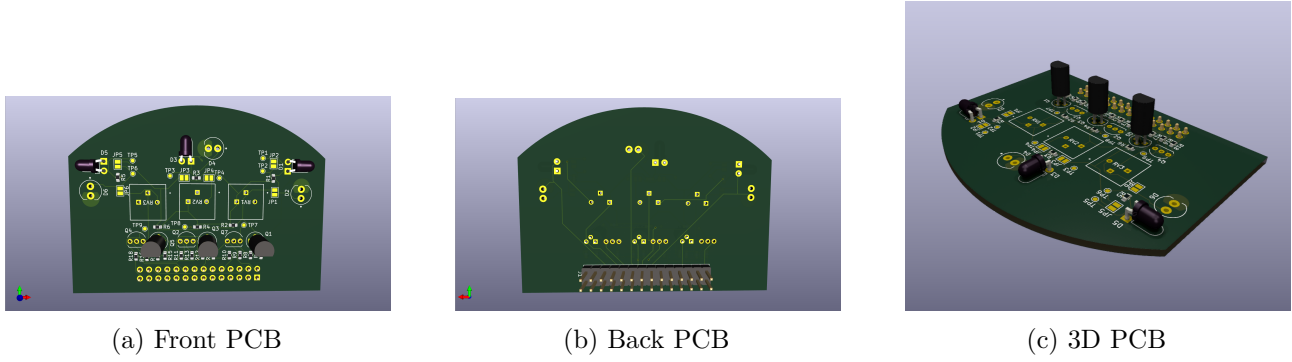


Figure 3.9: PCB

## 3.2 Failure Management

Table 3.4: Failure Management Processes

Failure Management Process	Description	Rationale
Jumpers for debugging	Jumpers were placed at strategic locations on the PCB.	<ul style="list-style-type: none"> <li>Jumpers allow for easy debugging and troubleshooting by providing access points to test and isolate different parts of the circuit.</li> <li>They could also be used as a means to place other components onto the PCB if needed.</li> </ul>
Test points for probing	Test points were included at critical nodes in the circuit.	<ul style="list-style-type: none"> <li>Test points facilitate probing and measuring signals at various stages of the circuit, aiding in diagnosing issues and verifying correct operation.</li> </ul>
Potentiometer jumper option	A jumper option was included to allow the connection of a potentiometer in parallel with the 10k resistor.	<ul style="list-style-type: none"> <li>The potentiometer provides adjustability for fine-tuning the circuit if needed.</li> <li>It was not populated to reduce costs but can be sourced from the White Lab if required.</li> </ul>

## 3.3 System Integration and Interfacing

### 3.3. System Integration and Interfacing

Table 3.5: Interfacing specifications

Interface	Description	Pinout/Output
I001	PWM signal from the processor to control the center ER Subsystem power	<ul style="list-style-type: none"> <li>STM32(PE13) to Pin 12 (on the 2x14 Connector) of the Sensing Subsystem</li> <li>STM32(GND) to GND Pin (on the 2x14 Connector) of the Sensing Subsystem</li> </ul>
I002	PWM signal from the processor to control the left ER sensor power	<ul style="list-style-type: none"> <li>STM32(PE15) to Pin 8 (on the 2x14 Connector) of the Sensing Subsystem</li> <li>STM32(GND) to GND Pin (on the 2x14 Connector) of the Sensing Subsystem</li> </ul>
I003	PWM signal from the processor to control the right ER sensor power	<ul style="list-style-type: none"> <li>STM32(PE11) to Pin 16 (on the 2x14 Connector) of the Sensing Subsystem</li> <li>STM32(GND) to GND Pin (on the 2x14 Connector) of the Sensing Subsystem</li> </ul>
I004	Digital output from the center Level Shifting Subsystem to the processor	<ul style="list-style-type: none"> <li>STM32(3V3) to 3V3 Pin (on the 2x14 Connector) of the Sensing Subsystem</li> <li>STM32(PE11) to Pin 14 (on the 2x14 Connector) of the Sensing Subsystem</li> <li>STM32(GND) to GND Pins (on the 2x14 Connector) of the Sensing Subsystem</li> </ul>
I005	Digital output from the left Level Shifting Subsystem to the processor	<ul style="list-style-type: none"> <li>STM32(3V3) to 3V3 Pin (on the 2x14 Connector) of the Sensing Subsystem</li> <li>STM32(PE14) to Pin 10 (on the 2x14 Connector) of the Sensing Subsystem</li> <li>STM32(GND) to GND Pin (on the 2x14 Connector) of the Sensing Subsystem</li> </ul>
I006	Digital output from the right Level Shifting Subsystem to the processor	<ul style="list-style-type: none"> <li>STM32(3V3) to 3V3 Pin (on the 2x14 Connector) of the Sensing Subsystem (on the 2x14 Connector) of the Sensing Subsystem</li> <li>STM32(PE10) to Pin 18 (on the 2x14 Connector) of the Sensing Subsystem</li> <li>STM32(GND) to GND Pin (on the 2x14 Connector) of the Sensing Subsystem</li> </ul>

**Note:**

- Any one of the following pins on the 2x14 Connector of the Sensing Subsystem can be used as ground: Pin 3, Pin 9, Pin 15, Pin 21, or Pin 27. Only one GND pin needs to be connected.
- Any one of the following pins on the 2x14 Connector of the Sensing Subsystem can be used as a 3V3 supply: Pin 2 or Pin 28. Only one 3V3 pin needs to be connected.

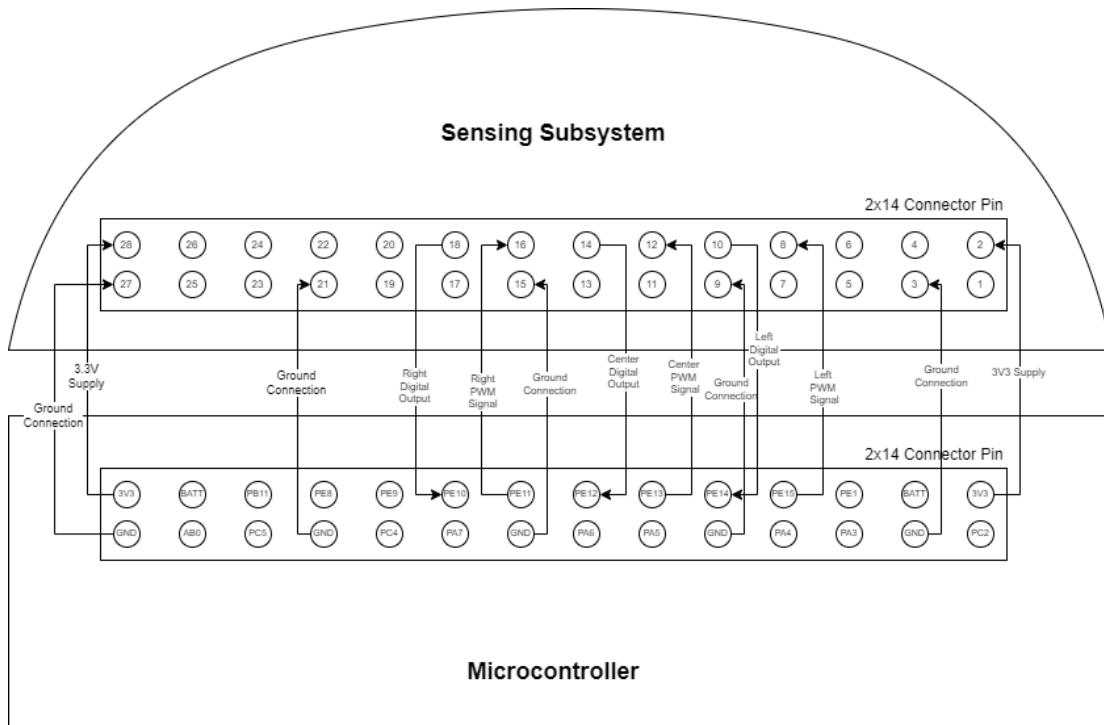


Figure 3.10: High Level Interfacing Diagram

# Chapter 4

## Acceptance Testing

### 4.1 Tests

Table 4.1: Subsystem acceptance tests

Test ID	Description	Testing Procedure	Pass/Fail Criteria
AT-01	Functionality test of the ER subsystems to verify that the sensors can detect walls within the specified range of 100mm to 200mm. This test ensures that the sensing subsystem meets the detection range requirements.	<ol style="list-style-type: none"> <li>Visually inspect the PCB for any manufacturing defects, poor soldering, or damaged components (a general inspection).</li> <li>Power on the sensing subsystem and verify that the IR emitters are functioning by viewing them through a camera or smartphone camera. The IR light should be visible on the camera display.</li> <li>Set up the micro-mouse in a controlled environment with adjustable walls.</li> <li>Place a wall at distances of 100mm, 150mm, and 200mm from each sensor (front, left, and right) and verify that the sensor detects its presence by observing a significant change in the output voltage at the corresponding test points (TP4, TP2, and TP6, respectively) compared to the no-obstacle condition.</li> </ol>	<p><b>Pass:</b> The PCB passes visual inspection, the IR emitters function correctly, and all ER subsystems detect the presence of walls at distances of 100mm, 150mm, and 200mm, as indicated by a significant change in output voltage at the corresponding test points compared to the no-obstacle condition.</p> <p><b>Fail:</b> The PCB fails visual inspection, the IR emitters do not function, or one or more ER subsystems fail to detect the presence of walls at any of the specified distances, with no significant change in output voltage compared to the no-obstacle condition.</p>
AT-02	Consistency test of the sensing subsystem's output voltage under varying environmental conditions (e.g., ambient light levels) using the analog to digital logic converter. This test verifies that the level shifter provides a consistent digital output (0V or 3.3V) based on the analog input, ensuring reliable wall detection minimally affected by environmental factors.	<ol style="list-style-type: none"> <li>Set up the micro-mouse in a controlled environment with a wall at a fixed distance (e.g., 150mm) from the front sensor.</li> <li>Measure the analog output voltage at TP4 and the digital output voltage at TP8 under normal ambient light conditions.</li> <li>Verify that the level shifter output at TP8 is approximately 3.3V when the analog voltage is above 0.7V and 0V when the analog voltage is below 0.7V.</li> <li>Vary the ambient light intensity (e.g., using a desk lamp or dimming the room lights) and repeat steps 2-3, ensuring that the level shifter output remains consistent.</li> <li>Repeat steps 2-4 for the left and right sensors, measuring the analog output voltage at TP2 and TP6, and the digital output voltage at TP7 and TP9, respectively.</li> </ol>	<p><b>Pass:</b> The level shifters consistently provide the correct digital output (0V or 3.3V) based on the analog input from the ER subsystems, ensuring reliable wall detection minimally affected by environmental factors.</p> <p><b>Fail:</b> The level shifters fail to provide consistent digital outputs based on the analog input from the ER subsystems, or the digital outputs vary significantly with changes in ambient light levels, indicating unreliable wall detection.</p>
AT-03	Functionality test of the sensing subsystem software to verify that it processes sensor data and indicates the presence of walls by toggling the corresponding LEDs (PB7, PB5, PB6) on the microcontroller. This test ensures that the software correctly interprets sensor data and communicates wall detection information.	<ol style="list-style-type: none"> <li>Set up the micro-mouse in a controlled environment with removable walls on the left, right, and front sides.</li> <li>Place a wall on the left side of the micro-mouse and verify that PB7 LED toggles on.</li> <li>Remove the left wall and verify that PB7 LED toggles off.</li> <li>Repeat steps 2-3 for the right side wall and PB5 LED.</li> <li>Repeat steps 2-3 for the front wall and PB6 LED.</li> </ol>	<p><b>Pass:</b> The LEDs (PB7, PB5, PB6) toggle correctly, indicating the presence or absence of walls on the left, right, and front sides, respectively.</p> <p><b>Fail:</b> One or more LEDs fail to toggle correctly based on the presence or absence of walls, indicating an issue with the sensing subsystem software.</p>
AT-04	Power consumption test of the sensing subsystem to verify that the PWM power-saving mechanism reduces power consumption by 50% or more compared to continuous operation. This test ensures that the sensing subsystem meets the power efficiency requirements.	<ol style="list-style-type: none"> <li>Measure the current consumption of the sensing subsystem during continuous operation (100% duty cycle) using an ammeter.</li> <li>Set the PWM duty cycle to 50% and measure the current consumption again.</li> <li>Calculate the percentage reduction in power consumption.</li> <li>Repeat steps 2-3 for duty cycles of 25% and 10%.</li> <li>Verify that the sensing subsystem still functions correctly at the reduced duty cycles by performing a basic wall detection test.</li> </ol>	<p><b>Pass:</b> The PWM power-saving mechanism reduces the current consumption of the sensing subsystem by 50% or more compared to continuous operation, and the sensing subsystem remains functional at the reduced duty cycles.</p> <p><b>Fail:</b> The PWM power-saving mechanism fails to reduce the current consumption by at least 50%, or the sensing subsystem does not function correctly at the reduced duty cycles.</p>
AT-05	Physical compatibility test to ensure that the sensing subsystem PCB fits within the specified dimensions (width <70mm, 6mm <length <50mm) and connects properly to the 2x14 pin header on the motherboard. This test verifies that the sensing subsystem meets the size and connectivity requirements.	<ol style="list-style-type: none"> <li>Measure the width of the sensing subsystem PCB at its widest point using a ruler or caliper.</li> <li>Measure the length of the sensing subsystem PCB from the edge of the 2x14 pin header to the opposite end.</li> <li>Verify that the width is less than 70mm and the length is between 6mm and 50mm.</li> <li>Connect the sensing subsystem PCB to the 2x14 pin header on the motherboard, ensuring that all pins are properly aligned.</li> <li>Gently tug on the sensing subsystem PCB to confirm that it is securely connected to the motherboard.</li> </ol>	<p><b>Pass:</b> The sensing subsystem PCB has a width less than 70mm, a length between 6mm and 50mm, and connects securely to the 2x14 pin header on the motherboard.</p> <p><b>Fail:</b> The sensing subsystem PCB exceeds the specified dimensions or does not connect properly to the 2x14 pin header on the motherboard.</p>

## 4.2 Critical Analysis of Testing

### 4.2.1 AT-01: Functionality Test of the ER Subsystems

During the initial testing of the ER subsystems (AT-01), several issues were discovered that significantly impacted the system's performance. Firstly, incorrect resistor values were used for the emitter circuits ( $R_1, R_3, R_5$ ) and the receiver circuits ( $R_2, R_4, R_6$ ). The emitter circuits used 100 resistors instead of the calculated 18 value, while the receiver circuits used 10k resistors instead of the intended 100k. These incorrect values led to suboptimal current flow and signal reception. Additionally, the testing revealed that powering the ER subsystems directly from the GPIO pins was not a viable solution, as the STM32 datasheet specifies a maximum current of 25mA per pin, which is insufficient for the required 100mA current for the IR emitters. To address this issue, the connections to the GPIO pins (PE15, PE13, PE11) were severed, and the ER subsystems were connected to the 3.7V battery (BATT) via pins 4 and 26 on the 2x14 connector.

During the testing phase, the IR emitters exhibited a faint light output, which was attributed to the use of the TSAL4400 model instead of the TSAL6100 used in the breadboard assignment. Moreover, no definitive output was observed at test points TP4, TP2, and TP6 when varying the distance of an object from the sensors. Further investigation revealed that the selected photodiode (SFH203PFA) had an upward sensing direction, rendering it unsuitable for the intended side-sensing application. To address these issues, the following actions were taken: all SFH203PFA photodiodes were replaced with the side-sensing SFH205FA model, and all TSAL4400 emitters were replaced with the brighter TSAL6100 model, both sourced from the White Lab. After these component replacements, the test was repeated, and the desired outputs were obtained: approximately 1.2V with no obstacle, 1.4V at 200mm, 1.7V at 150mm, and 2.2V at 100mm for all test points (TP4, TP2, TP6).

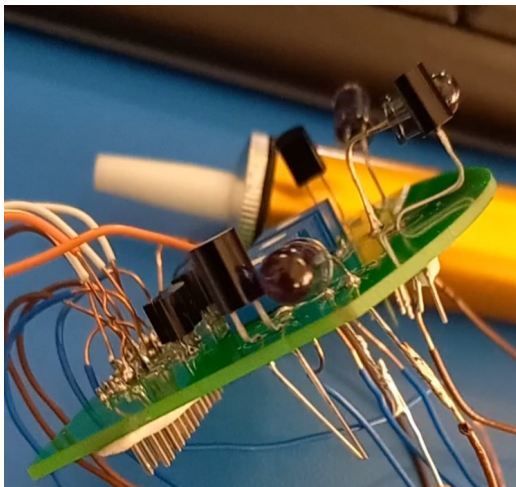


Figure 4.1: Image of IR emitting diode(TSAL6100) not working(off)

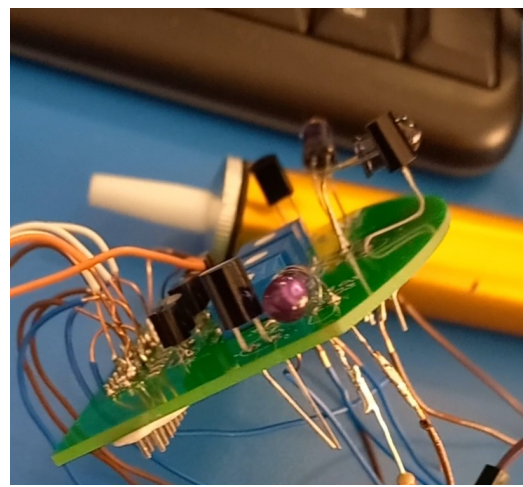


Figure 4.2: Image of IR emitting diode(TSAL6100) working(on)

These images show the sensing subsystem when the IR emitters are off (no purple light) and on (purple light visible), demonstrating that the IR sensing subsystem is functioning as intended.

These images show the multimeter readings of the analog output from one of the sensors. With no object present, the voltage is approximately 1.2V, while with an object, the voltage increases to 1.479V.

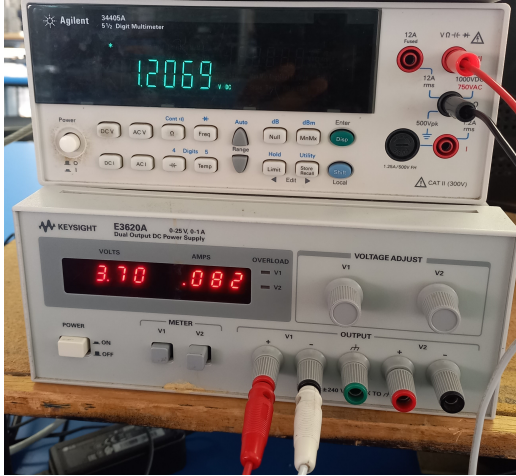


Figure 4.3: Multimeter and Power Supply readings when no object is detected

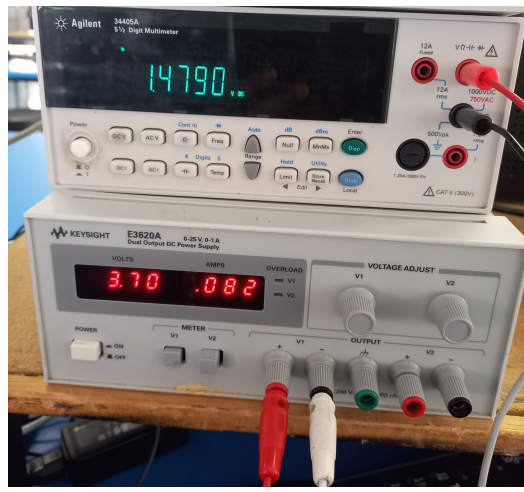


Figure 4.4: Multimeter and Power Supply readings for an object is detected

The power supply in both images shows a consistent 3.7V and 0.82A being drawn, confirming the stability of the power supply to the sensing subsystem.

The successful passing of AT-01 after these modifications highlights the importance of using the correct component values and models, as well as ensuring proper power supply and sensing direction for optimal performance of the ER subsystems.

#### 4.2.2 AT-02: Consistency Test of the Sensing Subsystem's Output Voltage

During the consistency test of the sensing subsystem's output voltage (AT-02), it was observed that the analog output voltages from the ER subsystems were consistently above 1V, even with varying distances of the object from the sensors. Specifically, the measured voltages were approximately 1.2V with no obstacle, 1.4V at 200mm, 1.7V at 150mm, and 2.2V at 100mm for all test points (TP4, TP2, TP6).

These high analog voltages posed a problem for the level shifter, which was designed to work with a threshold of around 0.7V. The potentiometer included on the board was considered as a potential solution for adjusting the voltage levels. However, it was determined that this approach would not be robust enough to account for real-world fluctuations in ambient lighting conditions.

To resolve this issue, the design was modified to connect the analog outputs directly to the ADC pins of the microcontroller (PA4, PA5, PA6) via pins 7, 11, and 13 on the 2x14 connector. This modification required severing the connections to the level shifter and soldering wires from test points TP2, TP6, and TP7 to pins 7, 11, and 13, respectively.

By utilizing the ADC, it became possible to capture and interpret the analog voltages programmatically, allowing for the implementation of a range of values that the circuit can work with to account for variations in ambient light. This modification meant that AT-02 could no longer be passed in its original form, but it ultimately led to a more adaptable and robust solution for handling the analog output voltages from the ER subsystems.

#### 4.2.3 AT-03: Functionality Test of the Sensing Subsystem Software

The change in approach from using a level shifter to an ADC necessitated significant modifications to the sensing subsystem software. Initially, the software was designed to receive digital outputs from the level shifter to toggle the LEDs (PB7, PB5, PB6) based on the presence or absence of a wall. However, with the ADC implementation, the software needed to be updated to read the analog values and determine the presence of a wall based on predefined thresholds. To facilitate the calibration process, an LCD was added to display the ADC values corresponding to the sensor outputs. This allowed for real-time monitoring and adjustment of the threshold values for each ER subsystem (left, right, and front).



Figure 4.5: PCB Sensing Subsystem dimensions

This image shows the LCD used to configure the ADC. The LCD screen displays the ADC value of one of the sensors and indicates that the LED is on, implying that the ADC value is triggering the LED to turn on. This evidence demonstrates the successful integration of the LCD for real-time monitoring and calibration of the sensing subsystem.

The testing procedure involved setting up the micro-mouse in a controlled environment and initially checking the LEDs for proper functionality. If an LED did not illuminate as expected, the corresponding ADC threshold value was recalibrated. The procedure included iteratively adjusting the threshold values for each ER subsystem, which were read through ADC channels PA4, PA5, and PA6, while monitoring the LED states and the ADC values displayed on the LCD.

This iterative calibration process was continued until the LEDs consistently toggled on and off based on the presence or absence of walls at the defined threshold values. The successful passing of AT-03 after this calibration procedure demonstrates the effectiveness of the revised software design in interpreting the analog sensor data and accurately detecting the presence of walls.

#### 4.2.4 AT-04: Power Consumption Test of the Sensing Subsystem

During the power consumption test (AT-04), it was discovered that sourcing PWM signals directly from the GPIO pins to control the power to the ER subsystems was not feasible due to current limitations. To mitigate this problem, a P-channel MOSFET was sourced from the White Lab and incorporated into the circuit. The P-channel MOSFET was configured with its source connected to the 3.7V battery (BATT), and its gate connected to a PWM-capable pin (PE15) of the microcontroller, which corresponds to pin 8 on the 2x14 connector. The drain of the MOSFET was then used as the voltage source for the ER subsystems, with a voltage close to 3.7V. Initial testing revealed that with all components connected (except for the level shifter), the current drawn by the system was

approximately 295mA, close to the expected 300mA (100mA for each of the three ER subsystems). Adjusting the PWM frequency to 1Hz resulted in a noticeable reduction in power consumption while still providing sufficient time for the IR emitters to illuminate and be detected by the sensors. However, it was observed that the analog output voltages at test points TP4, TP2, and TP6 were also affected by the PWM signal. To address this issue, the following modification was made: only the IR emitters were connected to the PWM-controlled voltage source (drain of the P-channel MOSFET), while the receivers (photodiodes) were powered directly from the 3.7V battery (BATT). This approach made sense conceptually, as the emitters are the primary current-drawing components, whereas the photodiodes only draw current when receiving reflected IR light. After implementing this modification, the testing procedure was repeated successfully, and a PWM duty cycle of 50% was selected as it provided an optimal balance between power savings and reliable wall detection, allowing sufficient time for the emitters to illuminate and the sensors to capture the reflected IR light.

#### 4.2.5 AT-05: Physical Compatibility Test

The physical compatibility test (AT-05) focused on ensuring that the sensing subsystem PCB fits within the specified dimensions and connects properly to the motherboard. The length of the PCB was measured to be 54mm, which was deemed optimal for preventing sensor obstruction by the wheels while maintaining a compact overall design.

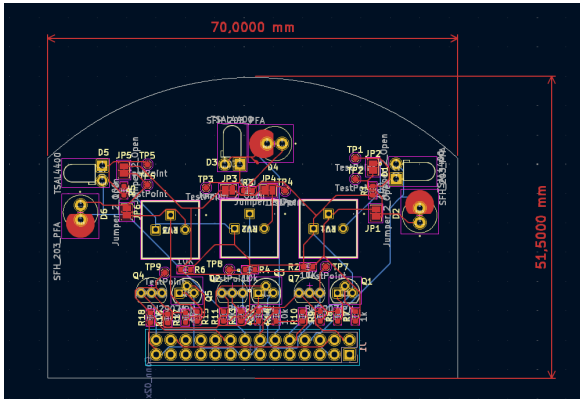


Figure 4.6: PCB Sensing Subsystem dimensions

This image shows the dimensions of the PCB as designed in KiCad, measuring 70mm x 51.5mm. These dimensions demonstrate that the sensing subsystem PCB was designed to fit properly within the specified constraints, ensuring compatibility with the micro-mouse platform.

During testing, the PCB was successfully connected to the motherboard using the appropriate 2x14 2.54mm pin header, and all connections were verified to be secure. The test was passed, confirming that the sensing subsystem PCB meets the physical compatibility requirements for integration with the micro-mouse platform.

The inclusion of the KiCad dimensions image provides additional evidence that the sensing subsystem PCB was designed with the specific dimensions in mind, further supporting the successful outcome of the physical compatibility test. This attention to detail in the design phase demonstrates a proactive approach to ensuring the proper fit and integration of the sensing subsystem with the overall micro-mouse platform.

# Chapter 5

## Conclusion

The sensing subsystem design project aimed to develop a reliable and efficient solution for wall detection, power management, and system integration in the micro-mouse robot. The motivation behind this project was to enable the micro-mouse to navigate a maze successfully while adhering to the specified requirements and constraints.

The final solution incorporated a combination of IR emitter-receiver pairs, an analog-to-digital converter (ADC), and pulse-width modulation (PWM) for power control. The design underwent several iterations and modifications based on the findings from the Acceptance Tests, which highlighted the importance of component selection, power management, and adaptable software design.

The most significant findings from the project include:

1. The transition from a level shifter to an ADC for processing analog sensor data improved the system's flexibility and robustness in handling variations in ambient light conditions.
2. Proper power management, achieved through the use of a P-channel MOSFET and PWM control, successfully reduced power consumption while maintaining reliable wall detection capabilities.
3. The physical compatibility test confirmed that the sensing subsystem PCB met the size and connectivity requirements for seamless integration with the micro-mouse platform.

The results obtained from the Acceptance Tests clearly support the effectiveness of the design decisions and modifications made throughout the project. The sensing subsystem successfully detected walls within the specified range, provided consistent output voltages, and demonstrated accurate wall detection through the integration of an LCD for real-time monitoring and calibration.

However, during the demonstration, the sensing subsystem's performance was adversely affected by drastically different lighting conditions compared to the one used for configuring the ADC range. This limitation highlighted the need for a more dynamic approach to calibration, such as the incorporation of a potentiometer to adjust the output and ensure that it falls back within the desired range. Although the PCB design included jumpers (JP2, JP4, and JP6) to connect the output to a potentiometer, this feature was not utilized during the demonstration, limiting the ability to adapt to varying light conditions in real-time.

In conclusion, the sensing subsystem design project successfully addressed the challenges of wall detection, power efficiency, and system integration, ultimately contributing to the development of a functional and reliable micro-mouse robot. The lessons learned from this project, such as the importance of iterative design, thorough testing, and attention to detail, will be valuable in future

engineering endeavors. However, the demonstration also revealed areas for improvement, particularly in terms of real-time adaptability to varying environmental conditions.

## 5.1 Recommendations

To further enhance the sensing subsystem and the overall micro-mouse project, the following recommendations are proposed:

1. **Utilize the potentiometer for ADC calibration:** To account for drastically different lighting conditions, the potentiometer should be connected to the output of the ER subsystems using jumpers JP2, JP4, and JP6. This will allow for real-time adjustment of the output voltage, ensuring that it falls within the desired range for accurate wall detection. By implementing this dynamic calibration approach, the sensing subsystem can adapt to varying environmental conditions without the need for manual code modifications.
2. **Investigate the use of advanced signal processing techniques or alternative IR receivers** to mitigate the impact of ambient light on the sensing subsystem's performance. Despite the SFH205's daylight blocking capabilities, the sensing subsystem's output still exhibited slight variations under different lighting conditions. Implementing hardware or software-based filtering techniques, such as band-pass filters, digital signal processing algorithms, or adaptive thresholding methods, could help isolate the desired IR signal from ambient noise. Additionally, researching and experimenting with alternative IR receivers offering enhanced ambient light rejection capabilities could further improve the system's resilience to lighting fluctuations.

By implementing these recommendations, the sensing subsystem can be further refined and optimized to achieve higher levels of performance, reliability, and adaptability. These enhancements will not only benefit the current micro-mouse project but also lay the foundation for future developments and innovations in the field of autonomous maze-solving robots. The lessons learned and the knowledge gained from this project can be applied to similar engineering challenges, fostering the growth and advancement of robotics and embedded systems engineering.

# Bibliography

R